HHS Public Access

Author manuscript

Circulation. Author manuscript; available in PMC 2019 October 09.

Published in final edited form as:

Circulation. 2018 October 09; 138(15): 1569–1581. doi:10.1161/CIRCULATIONAHA.118.034361.

Rearrangement of the Protein Phosphatase 1 Interactome during Heart Failure Progression

David Y. Chiang, MD, PhD[*,a,b,c], **Katherina M. Alsina, BA**[*,b,d], **Eleonora Corradini, PhD**[c,e], **Martin Fitzpatrick, PhD**[c,e], **Li Ni, MD, PhD**[b,f], **Satadru K. Lahiri, PhD**[b,f], **Julia Reynolds, BS**[f], **Xiaolu Pan, MD, MS**[f], **Larry Scott Jr, BS**[f], **Albert J.R. Heck, PhD**[^,c,e], and **Xander H.T. Wehrens, MD, PhD**[^,b,f,g,h]

[a]Department of Medicine, Brigham and Women's Hospital, Harvard Medical School, Boston, MA, USA [b]Cardiovascular Research Institute, Baylor College of Medicine, Houston, TX, USA [c]Biomolecular Mass Spectrometry and Proteomics, Bijvoet Center for Biomolecular Research and Utrecht Institute for Pharmaceutical Sciences, Utrecht University, Utrecht, The Netherlands [d]Integrative Molecular and Biomedical Sciences, Baylor College of Medicine, Houston, TX, USA [e]Netherlands Proteomics Centre, Utrecht, The Netherlands [f]Department of Molecular Physiology & Biophysics, Baylor College of Medicine, Houston, TX, USA [g]Department of Medicine (Cardiology), Baylor College of Medicine, Houston, TX, USA [h]Department of Pediatrics (Cardiology), Baylor College of Medicine, Houston, TX, USA

Abstract

Background—Heart failure (HF) is a complex disease with a rising prevalence despite advances in treatment. Protein phosphatase 1 (PP1) has long been implicated in HF pathogenesis but its exact role is both unclear and controversial. Most previous studies measured only the PP1 catalytic subunit (PP1c) without investigating its diverse set of interactors, which confer localization and substrate specificity to the holoenzyme. In this study we define the PP1 interactome in cardiac tissue and test the hypothesis that this interactome becomes rearranged during HF progression at the level of specific PP1c interactors.

Methods—Mice were subjected to transverse aortic constriction and grouped based on ejection fraction (EF) into sham, hypertrophy, moderate HF (EF 30–40%), and severe HF (EF<30%). Cardiac lysates were subjected to affinity-purification using anti-PP1c antibodies followed by high-resolution mass spectrometry. Ppp1r7 was knocked down in mouse cardiomyocytes and HeLa cells using adeno-associated virus serotype 9 (AAV9) and siRNA, respectively. Calcium imaging was performed on isolated ventricular myocytes.

Addresses for Correspondence: Albert Heck, PhD, Biomolecular Mass Spectrometry and Proteomics, Utrecht University, Padualaan 8, 3584 CH Utrecht, The Netherlands, Tel: (+31)030-253-6797, a.j.r.heck@uu.nl, Xander Wehrens, MD, PhD, Cardiovascular Research Institute, Baylor College of Medicine, BCM335, One Baylor Plaza, Houston, Texas 77030, Tel: (+1)713-798-4261, wehrens@bcm.edu.

*Co-first authors

^Co-corresponding authors

DISCLOSURES

Dr. Wehrens is a co-founder and co-owner of ELEX Biotech, a biotech company dedicated to the development of drug molecules that target RyR2 for the treatment of heart disease.

Results—Seventy-one and 98 PP1c interactors were quantified from mouse cardiac and HeLa lysates, respectively, including many novel interactors and protein complexes. This represents the largest reproducible PP1 interactome dataset ever captured from any tissue, including both primary and secondary/tertiary interactors. Nine PP1c interactors with changes in their binding to PP1c were strongly associated with HF progression including two known (Ppp1r7, Ppp1r18) and 7 novel interactors. Within the entire cardiac PP1 interactome, Ppp1r7 had the highest binding to PP1c. Cardiac-specific knockdown in mice led to cardiac dysfunction and disruption of calcium release from the sarcoplasmic reticulum.

Conclusions—PP1 is best studied at the level of its interactome, which undergoes significant rearrangement during HF progression. The nine key interactors that are associated with HF progression may represent potential targets in HF therapy. In particular, Ppp1r7 may play a central role in regulating the PP1 interactome by acting as a competitive molecular “sponge” of PP1c.

Keywords

protein phosphatase 1; PP1 regulatory subunits; PP1 interactors; interactome; Ppp1r7; heart failure; affinity purification; mass spectrometry; proteomics

INTRODUCTION

Heart failure (HF) is a complex disease with a rising prevalence globally.[1] Although HF may be caused by various primary etiologies, HF secondary to hypertension remains a major clinical challenge where the disease process likely starts long before the patients become symptomatic.[1,2] This progression of HF and its underlying molecular mechanisms remain poorly understood, despite advances in treatment to control risk factors such as hypertension.[1]

Protein phosphatase 1 (PP1) is one of the most abundant and ubiquitous serine/threonine phosphatases, and has long been implicated in a number of cardiac diseases including HF.[3–12] Whereas a number of studies suggest that increased PP1 activity contributes to HF development and that its global inhibition may be therapeutic,[4–8] other studies provided conflicting results[9–12] as recently reviewed.[3,13] Most studies to date considered PP1 as a single entity and only measured or manipulated its global level and/or activity. In reality, however, the PP1 holoenzyme is made up of a catalytic subunit (PP1c) and one (or sometimes two) regulatory (R)-subunits, which are part of a large set of approximately 200 putative PP1c interactors.[14] Because there are only four PP1c isoforms, subcellular localization and target specificity are largely determined by the specific R-subunits/interactors that bind to PP1c. In other words, PP1 should be studied as an integral part of an extensive and variable interactome. Only with such detailed understanding of the PP1 interactome can its contribution to HF pathogenesis be deciphered.

Here we applied high-resolution affinity purification-mass spectrometry (AP-MS), using specific anti-PP1c antibodies,[15] to study changes in the PP1 interactome of mice subjected to transverse aortic constriction (TAC) and subsequently progressed through different stages of HF. We established a robust and reproducible PP1 interactome in both mouse hearts and HeLa cell line using a generalizable protocol, identified numerous novel PP1c interactors

and quantified their relative binding to PP1c. We then identified a number of key alterations in this interactome during HF progression which may serve as potential therapeutic targets. Finally, we showed that protein phosphatase 1 regulatory subunit 7 (Ppp1r7) is a key PP1c interactor important for cardiac function *in vivo* and that it may do so by acting as a competitive "sponge" to other interactors. Altogether, our study unveils the complexity and dynamics of the PP1 interactome, identifies both novel and key interactors relevant to HF pathogenesis, and provides mechanistic insights into the rearrangement of the PP1 interactome via Ppp1r7.

METHODS

Detailed experimental protocols including data deposition are provided in the Online Supplement. The data, analytic methods, and study materials will be/have been made available to other researchers for purposes of reproducing the results or replicating the procedure. The MS proteomics data have been deposited in the ProteomeXchange Consortium via the PRIDE16 partner repository (identifier: PXD004643).

Study animals

Protocols were approved by the Institutional Animal Care and Use Committee of Baylor College of Medicine. Wild-type (WT) male C57BL/6 mice between the ages of 3–4 months were either sacrificed at baseline or subjected to transverse aortic constriction or sham surgery and followed by serial echocardiography before sacrifice. Their ventricles were harvested and immediately flash-frozen in liquid nitrogen. For virus studies, 2–3 month old αMHC WT and transgenic (TG) mice were anaesthetized prior to retro-orbital injection of either control (shScr) or experimental (shPpp1r7) adeno-associated viruses (AAV9).

Transverse aortic constriction

Surgeries were performed according to previously published protocols.[16] Sham surgeries were similarly performed but without constriction of the aorta.

Transthoracic echocardiography

Echocardiography was performed as previously described using the VisualSonics VeVo 770 Imaging System (VisualSonics, Toronto, Canada) equipped with high-frequency 30 MHz probe.[17]

Co-immunoprecipitation, gel electrophoresis and protein digestion

PP1c co-immunoprecipitation, gel electrophoresis and in-gel protein digestion were performed as previously described.[15]

Statistical analyses

Data are expressed as means ± standard error of the mean (SEM). Differences between two groups were evaluated by unpaired two-tailed Student's *t*-test whereas differences among more than two groups were evaluated by ANOVA followed by pairwise comparison tests. Adjusted p-values to correct for multiple comparisons were computed using the Sidak method. The alpha (α) level was set at 0.05.

RESULTS

Establishing the PP1 interactome in the mouse heart

In order to investigate the rearrangement of the PP1 interactome during HF progression, we first set out to establish a robust and reproducible PP1 interactome. Cardiac ventricles from 8 mice were pooled into 4 samples of 2 mice each. Each of the 4 pooled samples was subjected to parallel affinity purification using either highly selective anti-PP1c antibodies or nonspecific IgG antibodies as control. All immunoprecipitated proteins were qualitatively and quantitatively identified using liquid chromatography-mass spectrometry (Figure 1A). After stringent filtering, we identified 267 proteins of which 71 were significantly enriched in the PP1c immunoprecipitation (IP; Figure 1B; Supplemental Table 1). To gain insight into the abundance of each protein in the pull-down we quantified each protein using the well-established intensity based absolute quantification (iBAQ) method.[18] The bait PP1c (Ppp1ca) had the highest abundance in the pull-down, demonstrating the selectivity of the antibodies. At least 10 well known PP1c interactors, namely the various R-subunits, were also significantly enriched demonstrating the success of our IP. Only one known R-subunit, Ppp1r13b, fell below the stringent statistical cut-off (Figure 1B; FDR=0.01, s0=0.1), likely because it was detected at very low levels (Supplemental Table 1). Although these conservative cut-off criteria minimized false positives at the expense of missing occasional true positives (only one that we know of), they result in a robust and reproducible PP1 interactome, against which we can confidently benchmark further studies.

Since AP-MS identifies protein complexes in addition to primary interactors, we cross-referenced every protein in our newly defined PP1 interactome with the CCSB Human Interactome Database (http://interactome.dfci.harvard.edu/H_sapiens/), which is based on yeast two-hybrid (Y2H) studies mapping binary interactions (Figure 1D). Of the 71 proteins in the PP1 interactome, 22 proteins had at least one known binary interaction, clustering into at least 5 protein complexes (Figure 1E). The remaining 49 interactors were not catalogued and may represent novel and possible cardiac-specific interactors.

To further validate the level of enrichment achieved with the PP1c-IP, we performed MS analysis on two of the same WT lysates without IP. This resulted in 1804 quantifiable proteins that were ranked according to their abundance in the mouse heart based on iBAQ (Supplemental Figure 1A). For comparison, the same analysis was performed for the 71 enriched proteins from the PP1c AP-MS data (Supplemental Figure 1B). Forty-four of the 71 proteins were detected in the global proteome (Supplemental Table 2). Among the 21 that were not detected were Ppp1r2, Ppp1r11, Ppp1r8, Ppp1r18, Ppp1r12c, Ppp1r9b, Ppp1r12a, and Ppp1r13l (Supplemental Figure 1). This suggests that these proteins are low in abundance in the mouse heart, and were only detectable in our analysis after enrichment with PP1c. Some of the other known PP1 subunits such as Ppp1r12b, Ppp1r7, and the catalytic PP1 subunits were already detected in the “full” proteome but were more highly enriched with AP-MS (Supplemental Figure 1). Interestingly, Ppp1r14c was detected only in the global proteome analysis and not in the PP1c-IP, possibly because it has been reported to require phosphorylation by protein kinase A in order to bind PP1c.[19] This analysis

demonstrates and confirms the success of the enrichment achieved from the AP-MS experiments.

Mouse model of heart failure progression

Once we established a robust workflow to quantify the PP1 interactome, we applied it to study a well-characterized mouse model of HF progression, the TAC model. Mouse hearts were harvested at 2, 4, 6, and 8 weeks following either TAC or sham operation (Supplemental Figure 2A). The mice were grouped based on their ejection fraction (EF) determined by echocardiography. The Sham group consisted of mice that underwent a mock surgery and were harvested 2, 4, 6, or 8 weeks post-surgery in order to avoid potential confounding of time since surgery (6 mice per time point for a total of 24 mice; Supplemental Table 3). The hypertrophy (Hyp), moderate HF (mHF), and severe HF (sHF) groups consisted of 10 mice each with normal EF, EF between 30 and 40%, or EF<30% post-TAC, respectively. One mouse with an EF of 32% had echo and physiological parameters consistent with sHF and was grouped accordingly (Supplemental Table 3). As the animals developed HF based on final EF, their heart weight and lung weight (normalized to tibia length) increased significantly (Supplemental Figure 2B–D). Other echo parameters and physical characteristics of the animals are summarized in Supplemental Table 3.

Proteins associated with HF progression

Following collection of the mouse ventricles, samples were processed in parallel for PP1c AP-MS using the established workflow (Figure 2A), which resulted in 692 identified and quantified proteins (Supplemental Table 4). Of these we first sought to identify key proteins associated with HF progression, irrespective of whether they were part of the PP1 interactome. A model using partial least squares (PLS) regression was built from the label-free quantification (LFQ) intensities of all 692 proteins in order to predict the final EF for a given mouse by taking into account the abundance of the proteins quantified by AP-MS. Individual proteins were assigned weights which described the covariance between their abundance and the target variable (EF), and whether this relationship was positive or negative (Supplemental Table 5). A protein with a higher weight is more strongly associated with changes in EF. Based on this model, we were able to recapitulate the grouping of all 54 mice according to their earlier classifications (Figure 2B). The Hyp group clustered with the Sham group whereas the mHF and sHF groups clustered away from the Sham group, with the sHF group being the furthest away. All but 2 samples (1 Sham, 1 Hyp) clustered within the 95% CI for their respective group. This demonstrated that there were distinct differences in the AP-MS proteome during different stages of HF and that the proteomic data generated may be useful in predicting EF.

Of all the proteins used in the initial model, we were particularly interested in those that were most highly correlated with, or most predictive of, the final EF. Using a forward selection approach, we progressively added proteins in order of their PLS regression model weights. Improvement of the model was assessed by r^2 and proteins were added until reaching the inflection point where the performance of the model plateaued (Supplemental Figure 3). We defined a cut-off at this inflection point giving us a total of 40 proteins that were the top predictors of final EF in our model (Supplemental Table 5). Using these

proteins, we repeated the PLS regression clustering and obtained a similar separation of the groups (Figure 2C). Clustering was slightly poorer with 4 samples outside their respective 95% CI. However, we could still accurately predict the final EF in our experimental samples by using this limited set of 40 proteins (r^2=0.9, $p<0.01$). These proteins may represent key pathways or networks involved in the disease process (Supplemental Table 5).

Rearrangement of the PP1 interactome during HF progression

Of the 40 proteins most strongly associated with HF progression, 9 were part of the 71 PP1c interactors defined earlier, two of which are also known PP1 R-subunits: Ppp1r7 and Ppp1r18 (Figure 3A). Figure 3B shows the overlap between the global proteome (1804 proteins; Supplemental Figure 1A), PP1 interactome (71 proteins; Supplemental Figure 1B), and proteins associated with HF progression (40 proteins). While each of these datasets was informative by itself, the overlap was of particular interest because these proteins were 1) readily detectable in our system globally, 2) enriched with PP1c-IP, and 3) associated with HF progression. They include the following 7 proteins in descending order of their abundance in the proteome: Ppp1r7, Des, Dbt, Prrc1, Hnrnpm, Hsd17b8, and Bckdha (Figure 3B). The other two, Ppp1r18 and Ccdc85c, were not detected in the proteome but were enriched in the PP1 interactome and also associated with HF progression so may also be of interest for future studies. The levels of binding between these 9 proteins and PP1c during HF progression were plotted in Figure 3C in descending order of their abundance in the PP1 interactome.

Among the 9 interactors associated with HF progression, 5 had an increase in binding whereas 4 had a decrease in binding to PP1c during HF progression (Figure 3C). To assess whether these changes in binding to PP1c were secondary to global changes in their protein levels, we repeated the MS analysis with some of the same lysates but without PP1c-IP (Supplemental Figure 4). In total we quantified 1931 proteins, of which 553 were significantly changed during HF progression (Supplemental Table 6). Of these, 14 are among the 71 PP1c interactors and 32 were among the 40 key proteins associated with HF progression based on the PLS regression analysis (Supplemental Table 6). Five proteins were both significantly changed at the proteome level, PP1c interactors, and among the key proteins identified by PLS regression: Ppp1r7, Dbt, Prrc1, Hsd17b8, and Bckdha. Supplemental Table 7 summarizes the relative changes of these interactors in terms of their levels of binding to PP1c, their global protein abundance, and their global protein level relative to the global level of PP1c in the sHF group compared to the Sham group. Among this group of select proteins, the global changes relative to PP1c were consistent with the changes in binding to PP1c for 4 of the proteins: Dbt, Prrc1, Bckdha, and Hsd17b8. This suggests that the changes in their binding to PP1c during HF progression may be partially explained by changes in their global protein expression (relative to that of PP1c). However, for Ppp1r7, there was no change in its global level relative to that of PP1c during HF progression, yet its binding to PP1c was increased. This implies that another mechanism may be responsible for the increase in binding (Supplemental Table 7).

The role of Ppp1r7 during HF progression

In order to validate this finding for Ppp1r7 and to further investigate its role in HF progression, we performed western blots on lysates from the 4 groups of mice (Figure 4). The protein levels of both Ppp1r7 and PP1c increased with HF progression when normalized to calsequestrin (CSQ) or total protein input (Figure 4). However, when the level of Ppp1r7 was normalized to that of PP1c, there was no significant change in its level during HF progression (Figure 4C). This validates the MS findings that even though the level of Ppp1r7 bound to PP1c increased with HF progression (Figure 3C), the relative abundance of Ppp1r7 to PP1c was unchanged (Supplemental Table 7).

To determine whether the increased interaction between PP1c and Ppp1r7 in HF was pathogenic or compensatory, we generated a mouse model with cardiac-specific knock-down of Ppp1r7 using shRNA targeting Ppp1r7 (shPpp1r7) versus a scramble shRNA (shScr), delivered via adeno-associated virus serotype 9 (AAV9; Supplemental Figure 5A–B). Cardiac-specific knockdown was achieved using AAV9 vectors containing a loxP-flanked transcriptional stop cassette that prevents expression of the shRNA sequence in the absence of Cre recombinase. Either shPpp1r7-AAV9 or shScr-AAV9 was injected into mice expressing a constitutively active, cardiac-specific Cre (αMHC TG mice), and for both viruses overall transduction efficiency in ventricular myocytes was around 70% (Supplemental Figure 5C–D). Approximately 25% knock-down of Ppp1r7 was achieved (1.00±0.04 vs. 0.74±0.05, $p<0.05$) without compensatory changes in global PP1c level (1.00±0.23 vs. 0.9±0.05, p=N.S; Supplemental Figure 5D–E). Ventricular function of these mice was evaluated using echocardiography at baseline and at 2, 4, 6, and 8 weeks after AAV9 injection, demonstrating a gradual decline in EF that is modest but significant at 6 and 8 weeks. Moreover, a corresponding increase in end-systolic diameter was significant at 8 weeks when comparing shPpp1r7 mice to shScr mice (Figure 5). As an additional control, WT mice were also injected with shScr-AAV9 but there was no significant difference compared with TG mice injected with shScr-AAV9. These and other echocardiography parameters are shown in Supplemental Table 8. Thus, lowering expression of Ppp1r7 led to the development of cardiac dysfunction.

To further characterize the functional effects of Ppp1r7 knockdown at the level of individual cardiomyocytes, ventricular myocytes were isolated from these mice for calcium (Ca) imaging. Figure 6 shows that compared to cells isolated from shScr mice, shPpp1r7 cells had an increase in Ca sparks frequency (CaSF; 1.52±0.26 vs. 3.17±0.47; $p<0.05$), unaltered sarcoplasmic reticulum Ca loading (SR load; 2.26±0.29 vs. 1.79±0.33; p=N.S.), and an increase in CaSF normalized to SR load (1.22±0.34 vs. 2.76±0.58; $p<0.05$). Additional sparks characteristics are listed in Supplemental Table 9. Together, these data reveal that Ppp1r7 plays an essential role in cardiac function, and suggest that its increased binding to PP1c during HF progression may be compensatory rather than pathogenic.

Remodeling of the PP1 interactome induced by PPP1R7 knockdown

In order to determine the mechanism by which Ppp1r7 affects the PP1 interactome, we first noted that Ppp1r7 was the most highly bound PP1c interactor, by orders of magnitude, and therefore likely occupying the majority of PP1c molecules in the cytoplasm (Supplemental

Figure 1B). We therefore hypothesized that Ppp1r7 may be either an integral adaptor protein necessary for the binding of other interactors or a molecular “sponge” that competitively sequesters available PP1c, or both. To test this we first established the PP1 interactome in HeLa cells, which also express PP1c and PPP1R7 at high levels (Supplemental Figure 6A).[20] From this we quantified 155 proteins, 98 of which were significantly enriched in the PP1c vs. IgG-IP, including many known PP1 R-subunits (red; Supplemental Figure 6B; Supplemental Table 10). Supplemental Figure 6C shows the same proteins with their relative abundance, which shows PPP1CA with the highest abundance along with a number of known PP1 R-subunits. One notable difference from the mouse hearts was that PPP1R8 was the most abundant interactor, with PPP1R7 being second (Figure 1C; Supplemental Figure 6C). Moreover, due to the better-controlled conditions in cell culture we were able to recover more putative interactors in HeLa cells than from the mouse hearts. Since HeLa cells are widely used, the characterization of its PP1 interactome will be useful to future studies. As before we cross-referenced every protein in the newly defined HeLa PP1 interactome with the CCSB Human Interactome Database (http://interactome.dfci.harvard.edu/H_sapiens/; Supplemental Figure 6D). Of the 98 proteins in the PP1 interactome, 32 proteins had at least one known binary interaction, suggesting at least 8 protein complexes (Supplemental Figure 6E). The remaining 66 were not catalogued in the Y2H databases and may represent novel interactions.

Once we established a robust PP1 interactome in HeLa cells, we knocked-down PPP1R7 using siRNA before performing AP-MS experiments to investigate its effect on the PP1 interactome (Figure 7A). Western blot shows that PPP1R7 was knocked-down ~70% without affecting global PP1c levels ($p<0.001$; Figure 7B–C). Figure 7D plots the relative changes in the interactors from the PP1c AP-MS with PPP1R7 knockdown (Supplemental Table 11). This analysis showed that there was a general increase in almost all of the other interactors, supporting the hypothesis that PPP1R7 serves as a competitive molecular “sponge”. On the other hand, there were a few proteins that had a decreased level, most notably UXT, YBX3 (also known as CSDA), and TPRN, all of which may depend on PPP1R7 for indirect binding to PP1c. Finally, proteins that were in the same complexes based on Y2H analyses (Supplemental Figure 6D–E) all changed in the same direction as expected (same symbols in Figure 7D). These findings support the notion that PPP1R7 regulates the PP1 interactome globally by competitively sequestering PP1c molecules.

DISCUSSION

In this study, we established a robust and reproducible PP1 interactome using AP-MS and identified 71 and 98 putative PP1c interactors from mouse cardiac tissues and HeLa cells, respectively, most of which have not been previously reported (Figures 1 and 7; Supplemental Tables 1 and 10). Next, using the well-established TAC mouse model, we showed that the PP1 interactome becomes rearranged in HF. Our studies identified 40 key proteins that strongly associated with HF progression, 9 of which are also PP1c interactors (Figures 2–3; Supplemental Tables 4–6). Of these, Ppp1r7 has the highest binding to PP1c in mouse ventricles and its knockdown *in vivo* led to the development of cardiac dysfunction in adult mice and increased Ca sparks in isolated ventricular myocytes (Figures 5–6). Using HeLa cells we showed that Ppp1r7 regulates the PP1 interactome by acting as a competitive

"sponge" of PP1c (Figure 7; Supplemental Table 11). Together our study suggests that Ppp1r7 plays an essential role in cardiac function by regulating the PP1 interactome, which becomes rearranged during HF progression.

New approaches in studying PP1

Dysregulation of protein phosphorylation is an important mechanism that underlies numerous diseases including atrial fibrillation (AF) and HF.[3,21–23] Whereas a number of studies have investigated the pathogenic role of protein kinases and developed pharmacologic interventions, relatively few studies have done the same for protein phosphatases.[3] This may be because protein kinases are widely diverse and thereby specific in their subcellular localization and substrate selection, making them ideal targets for pharmacologic interventions. By contrast, protein phosphatases are highly homologous in their catalytic subunits and instead depend on their R-subunits or interactors to achieve the same functional specificity.[14] Although this extra layer of complexity creates additional challenges to their study, it holds the key to unexplored opportunities for novel drug design. This concept was nicely demonstrated by a recent study in which a small molecule, guanabenz, selectively disrupted the interaction between PP1c and PPP1R15A (also known as GADD34), thereby preventing PP1's stress-induced dephosphorylation of the α-subunit of translation initiation factor 2 and rescuing the cells from protein misfolding stress.[24]

In terms of cardiovascular diseases such as HF, significant controversy exists surrounding the exact role(s) of PP1, as recently reviewed.[3,13] This may be due to the fact that most previous studies considered PP1 as a single enzyme without adequately addressing its interactome. With this in mind, we previously undertook a large-scale unbiased study in order to map changes in the PP1 interactome in AF,[15] which study became the basis of the current study. However, the major limitation of that study was that a single AP-MS run was used to map the PP1 interactome in mouse ventricles and another one in human atria.[15] The current study was designed to provide a more robust and reproducible PP1 interactome, against which future studies may be benchmarked. To this end we used 4 biological replicates as well as stringent statistical cut-offs to map the PP1 interactomes for both mouse ventricles and HeLa cells (Figure 1A–C and Supplemental Figure 6A–C). Furthermore, we cross referenced each putative interactor against all others in the CCSB Human Interactome Database in order to identify interactors that belong to the same protein complexes (Figure 1D–E and Supplemental Figure 6D–E). The limited numbers of complexes identified (5 and 8 for mouse ventricles and HeLa cells respectively) may be due to the fact that large-scale Y2H screens have relatively low sensitivity, or that most of the interactors identified in our AP-MS are secondary/tertiary interactors, or both. Also, one limitation inherent of AP-MS is that these interactions were captured in homogenates so may not completely recapitulate the interactome *in vivo*, although specific care was taken to preserve native conditions. In any case, we believe that this novel approach and the high quality datasets produced in this study will be invaluable not only to the cardiovascular field but also to the scientific community in general.

Novel Findings and Potential Clinical Implications

Besides generating a number of rich datasets, the present study produced a number of significant findings in understanding HF progression. First, we identified a set of 40 proteins whose bindings to PP1c are strongly associated with HF progression (Supplemental Table 5; Figure 2B–C). In fact, the binding of these proteins to PP1c changed consistently during HF progression and may be used to predict the EF of the animal. Although they may be impractical as clinical biomarkers since their levels are measured after PP1c-IP, they may represent key proteins, pathways or networks that are involved in disease progression.

Among this group of 40, 9 are of particular interest because they are either known (Ppp1r7 and Ppp1r18) or putative (Des, Dbt, Prrc1, Ccdc85c, Hnrnpm, Hsd17b8, Bckdha) interactors based on our newly defined PP1 interactome (Figure 3). To understand why the binding of these proteins to PP1c either increased or decreased during HF progression, we compared the level of their binding first to their global changes and then to their global changes relative to PP1c's global changes during HF progression (Supplemental Table 7). For 4 of the proteins (Dbt, Prrc1, Bckdha, and Hsd17b8), the changes in their binding to PP1c corresponded to their global changes relative to PP1c. In other words, their increase or decrease in PP1c binding is at least partially explained by their global increase or decrease. However, this was not the case for Ppp1r7 where there was no relative global increase (compared to PP1c which was also increased globally). In other words, the increase in Ppp1r7's binding to PP1c cannot be accounted for by its global expression changes. Interestingly this was the same finding in patients with paroxysmal AF where PPP1R7 was also increased in its binding to PP1c without significant global increase relative to PP1c.[15]

To explore the role of Ppp1r7 *in vivo* we knocked down Ppp1r7 in mouse cardiomyocytes, which resulted in cardiac dysfunction in mice and increased Ca sparks in isolated ventricular myocytes, even though the total knockdown level was modest (~25%; Figures 5–6). Since Ca sparks are directly related to SR Ca release via the ryanodine receptor type-2 (RyR2), increased CaSF normalized to SR load implies RyR2 hyperactivity, a mechanism which has previously been shown to underlie several cardiac diseases including HF.[22] This implies that Ppp1r7 knockdown may either directly or indirectly lead to RyR2 hyperactivity and HF in our model and that its increased interaction with PP1c found during HF progression may be compensatory rather than pathogenic.

Since Ppp1r7 is the top interactor of PP1c by a considerable amount in mouse ventricles (Supplemental Figure 1B), we theorized that it may either act as a necessary adaptor protein for other interactors or a competitive "sponge" that sequesters available PP1c. When we knocked-down PPP1R7 in HeLa cells, the majority of putative PP1c interactors were increased in their binding to PP1c, suggesting a competitive process with PPP1R7 (Figure 7). Therefore, the increase in binding between Ppp1r7 and PP1c during HF progression (Figure 3) (and in AF[15]) may lead to a decrease in binding of many other interactors and thereby affect phosphorylation of downstream targets. This makes Ppp1r7 an attractive therapeutic target although future studies are needed to further characterize its role(s) in HF progression.

On the other hand, PPP1R7 may also act as an adaptor protein for some of the interactors since a few of those had a decrease in their PP1c binding with PPP1R7 knockdown (Figure 7). Interestingly, the binding between PP1c and YBX3 (aka CSDA) was decreased (although non-significantly), suggesting that CSDA may bind to PP1c secondarily through PPP1R7 (Figure 7D). If this is the case, our previous finding of the increase in PP1c-CSDA binding in paroxysmal AF may actually be secondary to the increase in the PP1c-PPP1R7 binding where CSDA was not a primary interactor as suggested.[15] In any case, further work is needed to clarify this interaction, which may have potential implications in disease.

Conclusions

By applying state-of-the-art affinity purification-mass spectrometry methods, we have established the most complete PP1 interactome to date in both mouse hearts and HeLa cells. Our studies identified key PP1c interactors that were altered in their binding to PP1c during heart failure progression. In particular, we showed that Ppp1r7 may play a central role during cardiac remodeling by acting as a competitive “sponge” of PP1c. Altogether this study contributes multiple rich datasets and mechanistic insights into our understanding of the rearrangement of PP1 interactome during HF progression.

Supplementary Material

Refer to Web version on PubMed Central for supplementary material.

Acknowledgments

SOURCES OF FUNDING

This work was supported by the Basic Research Fellowship from the European Society of Cardiology (D.Y.C.), The Netherlands Organization for Scientific Research (NWO) via the Roadmap Initiative Proteins@Work (project number 184.032.201) (A.J.R.H.), the European Union Horizon 2020 programme FET-OPEN project MSmed (project number 686547) (A.J.R.H.), and National Institutes of Health grants R01-HL089598, R01-HL091947, and R01-HL117641 (X.H.T.W.), and American Heart Association grant 13EIA14560061 (X.H.T.W.).

LIST OF ABBREVIATIONS

AAV9	Adeno-associated virus serotype 9
AP-MS	Affinity purification-mass spectrometry
CaSF	Calcium sparks frequency
EF	Ejection fraction
HF	Heart failure
Hyp	Hypertrophy
iBAQ	Intensity based absolute quantification
IP	Immunoprecipitation
LFQ	Label-free quantification

mHF	Moderate heart failure
MS	Mass spectrometry
PLS	Partial least squares
PP1	Protein phosphatase 1
PP1c	Protein phosphatase 1 catalytic subunit
Ppp1r7	Protein phosphatase 1 regulatory subunit 7
R-subunit	Regulatory subunit
RyR2	Ryanodine receptor type-2
sHF	Severe heart failure
shPpp1r7	shRNA targeting Ppp1r7
shScr	Scramble shRNA
SR	Sarcoplasmic reticulum
TAC	Transverse aortic constriction
TG	Transgenic
WT	Wild-type
Y2H	Yeast two-hybrid

References

1. Ziaeian B, Fonarow GC. Epidemiology and aetiology of heart failure. Nat Rev Cardiol [Internet]. 2016; 13:368–378. Available from: DOI: 10.1038/nrcardio.2016.25
2. Mann DL, Bristow MR. Mechanisms and models in heart failure: The biomechanical model and beyond. Circulation. 2005; 111:2837–2849. [PubMed: 15927992]
3. Weber S, Meyer-Roxlau S, Wagner M, Dobrev D, El-Armouche A. Counteracting protein kinase activity in the heart: The multiple roles of protein phosphatases. Front Pharmacol. 2015; 6:1–19. [PubMed: 25805991]
4. Carr AN, Schmidt AG, Suzuki Y, del Monte F, Sato Y, Lanner C, Breeden K, Jing S-L, Allen PB, Greengard P, Yatani A, Hoit BD, Grupp IL, Hajjar RJ, DePaoli-Roach AA, Kranias EG. Type 1 phosphatase, a negative regulator of cardiac function. Mol Cell Biol. 2002; 22:4124–35. [PubMed: 12024026]
5. Pathak A, Del Monte F, Zhao W, Schultz JEl, Lorenz JN, Bodi I, Weiser D, Hahn H, Carr AN, Syed F, Mavila N, Jha L, Qian J, Marreez Y, Chen G, McGraw DW, Heist EK, Guerrero JL, DePaoli-Roach AA, Hajjar RJ, Kranias EG. Enhancement of cardiac function and suppression of heart failure progression by inhibition of protein phosphatase. Circ Res. 2005; 96:756–766. [PubMed: 15746443]
6. Nicolaou P, Rodriguez P, Ren X, Zhou X, Qian J, Sadayappan S, Mitton B, Pathak A, Robbins J, Hajjar RJ, Jones K, Kranias EG. Inducible Expression of Active Protein Phosphatase-1 Inhibitor-1 Enhances Basal Cardiac Function and Protects Against Ischemia/Reperfusion Injury. Circ Res. 2009; 104:1012–1020. [PubMed: 19299645]

7. Kirchhefer U, Baba HA, Bokník P, Breeden KM, Mavila N, Brüchert N, Justus I, Matus M, Schmitz W, DePaoli-Roach AA, Neumann J. Enhanced cardiac function in mice overexpressing protein phosphatase Inhibitor-2. Cardiovasc Res. 2005; 68:98–108. [PubMed: 15975567]
8. Brüchert N, Mavila N, Boknik P, Baba HA, Fabritz L, Gergs U, Kirchhefer U, Kirchhof P, Matus M, Schmitz W, DePaoli-Roach AA, Neumann J. Inhibitor-2 prevents protein phosphatase 1-induced cardiac hypertrophy and mortality. Am J Physiol Heart Circ Physiol. 2008; 295:H1539–46. [PubMed: 18689497]
9. El-Armouche A, Wittköpper K, Degenhardt F, Weinberger F, Didié M, Melnychenko I, Grimm M, Peeck M, Zimmermann WH, Unsöld B, Hasenfuss G, Dobrev D, Eschenhagen T. Phosphatase inhibitor-1-deficient mice are protected from catecholamine-induced arrhythmias and myocardial hypertrophy. Cardiovasc Res. 2008; 80:396–406. [PubMed: 18689792]
10. Grote-Wessels S, Baba HA, Boknik P, El-Armouche A, Fabritz L, Gillmann HJ, Kucerova D, Matus M, Müller FU, Neumann J, Schmitz M, Stümpel F, Theilmeier G, Wohlschlaeger J, Schmitz W, Kirchhefer U. Inhibition of protein phosphatase 1 by inhibitor-2 exacerbates progression of cardiac failure in a model with pressure overload. Cardiovasc Res. 2008; 79:464–471. [PubMed: 18453636]
11. Ladilov Y, Maxeiner H, Wolf C, Schäfer C, Meuter K, Piper HM. Role of protein phosphatases in hypoxic preconditioning. Am J Physiol Heart Circ Physiol [Internet]. 2002; 283:H1092–8. Available from: http://www.ncbi.nlm.nih.gov/pubmed/12181139.
12. Wittköpper K, Fabritz L, Neef S, Ort KR, Grefe C, Unsöld B, Kirchhof P, Maier LS, Hasenfuss G, Dobrev D, Eschenhagen T, El-Armouche A. Constitutively active phosphatase inhibitor-1 improves cardiac contractility in young mice but is deleterious after catecholaminergic stress and with aging. J Clin Invest [Internet]. 2010; 120:617–26. Available from: http://www.ncbi.nlm.nih.gov/pubmed/20071777.
13. Chiang DY, Heck AJR, Dobrev D, Wehrens XHT. Regulating the regulator: Insights into the cardiac protein phosphatase 1 interactome. J Mol Cell Cardiol. 2016; 101:165–172. [PubMed: 27663175]
14. Heroes E, Lesage B, Görnemann J, Beullens M, Van Meervelt L, Bollen M. The PP1 binding code: A molecular-lego strategy that governs specificity. FEBS J. 2013; 280:584–595. [PubMed: 22360570]
15. Chiang DY, Lebesgue N, Beavers DL, Alsina KM, Damen JMA, Voigt N, Dobrev D, Wehrens XHT, Scholten A. Alterations in the interactome of serine/threonine protein phosphatase type-1 in atrial fibrillation patients. J Am Coll Cardiol. 2015; 65:163–173. [PubMed: 25593058]
16. deAlmeida AC, van Oort RJ, Wehrens XHT. Transverse aortic constriction in mice. J Vis Exp [Internet]. 2010; 38:1729. Available from: http://www.ncbi.nlm.nih.gov/pubmed/20410870.
17. Respress JL, Wehrens XHT. Transthoracic echocardiography in mice. J Vis Exp [Internet]. 2010; 39:1738. Available from: http://www.ncbi.nlm.nih.gov/pubmed/20517201.
18. Schaab C, Geiger T, Stoehr G, Cox J, Mann M. Analysis of High Accuracy, Quantitative Proteomics Data in the MaxQB Database. Mol Cell Proteomics [Internet]. 2012; 11 M111.014068. Available from: http://www.mcponline.org/lookup/doi/10.1074/mcp.M111.014068.
19. Erdodi F, Kiss E, Walsh MP, Stefansson B, Deng JT, Eto M, Brautigan DL, Hartshorne DJ. Phosphorylation of protein phosphatase type-1 inhibitory proteins by integrin-linked kinase and cyclic nucleotide-dependent protein kinases. Biochem Biophys Res Commun. 2003; 306:382–387. [PubMed: 12804574]
20. Geiger T, Wehner A, Schaab C, Cox J, Mann M. Comparative Proteomic Analysis of Eleven Common Cell Lines Reveals Ubiquitous but Varying Expression of Most Proteins. Mol Cell Proteomics [Internet]. 2012; 11 M111.014050. Available from: http://www.mcponline.org/lookup/doi/10.1074/mcp.M111.014050.
21. Li N, Chiang DY, Wang S, Wang Q, Sun L, Voigt N, Respress JL, Ather S, Skapura DG, Jordan VK, Horrigan FT, Schmitz W, Müller FU, Valderrabano M, Nattel S, Dobrev D, Wehrens XHT. Ryanodine receptor-mediated calcium leak drives progressive development of an atrial fibrillation substrate in a transgenic mouse model. Circulation. 2014; 129:1276–1285. [PubMed: 24398018]
22. Respress JL, Van Oort RJ, Li N, Rolim N, Dixit SS, Dealmeida A, Voigt N, Lawrence WS, Skapura DG, Skårdal K, Wisløff U, Wieland T, Ai X, Pogwizd SM, Dobrev D, Wehrens XHT.

Role of RyR2 phosphorylation at S2814 during heart failure progression. Circ Res. 2012; 110:1474–1483. [PubMed: 22511749]

23. Chelu MG, Sarma S, Sood S, Wang S, Van Oort RJ, Skapura DG, Li N, Santonastasi M, Müller FU, Schmitz W, Schotten U, Anderson ME, Valderrábano M, Dobrev D, Wehrens XHT. Calmodulin kinase II-mediated sarcoplasmic reticulum Ca2+leak promotes atrial fibrillation in mice. J Clin Invest. 2009; 119:1940–1951. [PubMed: 19603549]
24. Tsaytler P, Harding HP, Ron D, Bertolotti A. Selective inhibition of a regulatory subunit of protein phosphatase 1 restores proteostasis. Science (80-). 2011; 332:91–94.

CLINICAL PERSPECTIVE

What is new?

- Heart failure (HF) caused by long-standing hypertension is a progressive disease but the underlying molecular mechanisms are not well understood.
- We developed a novel and unbiased way to comprehensively study protein phosphatase 1 (PP1) interactors in a mouse model of progressive heart failure induced by elevated afterload.
- Nine specific PP1 interactors were strongly associated with HF progression.
- Among these, Ppp1r7 was shown to play a central role in regulating the PP1 interactome by acting as a competitive molecular “sponge” of PP1.

What are the clinical implications?

- By developing a novel way to examine the bindings partners of protein phosphatase 1 (the PP1 interactome), we were able to simultaneously interrogate multiple pathways relevant to HF pathogenesis.
- The nine key PP1 interactors identified in our study are highly associated with HF progression.
- Moreover, PP1 regulatory subunit 7 (Ppp1r7) was shown to play a central role in heart failure progression.
- Understanding of molecular pathways associated with PP1 subunits may pave the way for early pharmacologic intervention to forestall the progression of HF.

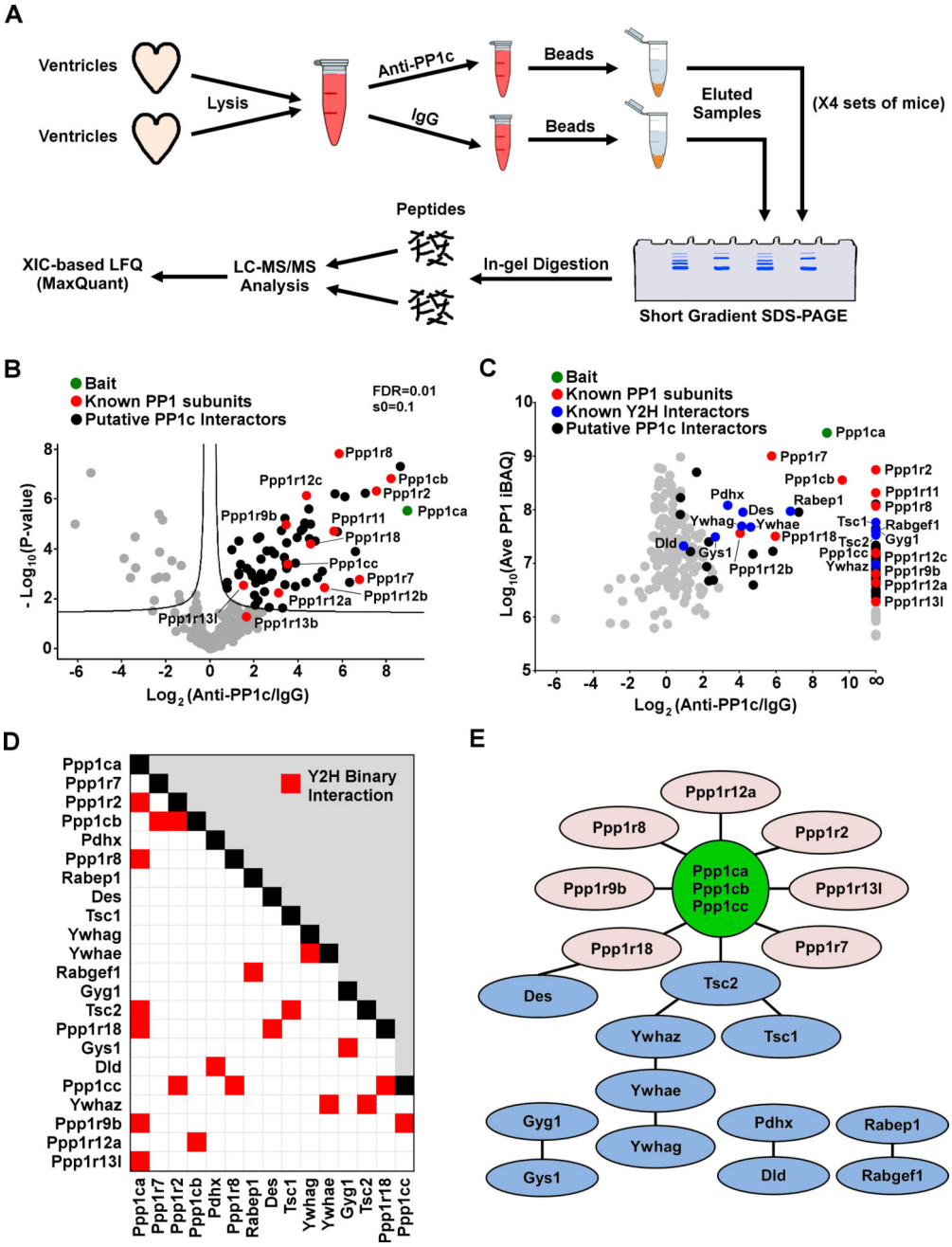

Figure 1. Establishing the PP1 interactome in the mouse heart

A. Overview of the experimental work-flow. LC-MS/MS=liquid chromatography-tandem mass spectrometry; XIC=extracted ion chromatogram; LFQ=label free quantitation. **B.** Volcano-plot showing that out of 267 identified and quantified proteins, 71 were significantly enriched in the PP1c vs. IgG-IP, including many known PP1 subunits (red). **C.** MA-plot showing the relative enrichment of proteins in the PP1c vs. IgG-IP where the highlighted proteins were statistically significant based on the volcano-plot in (**B**). Known binary interactors of PP1c based on yeast two-hybrid (Y2H) databases are in blue (besides the known PP1 subunits which are in red). Proteins with an infinite ratio (∞) have no LFQ

signals from the IgG-IP. **D–E.** Binary interactions among the 70 enriched proteins based on Y2H databases. Green=PP1 catalytic subunits; pink=known PP1 R-subunits; blue=other PP1 interactors.

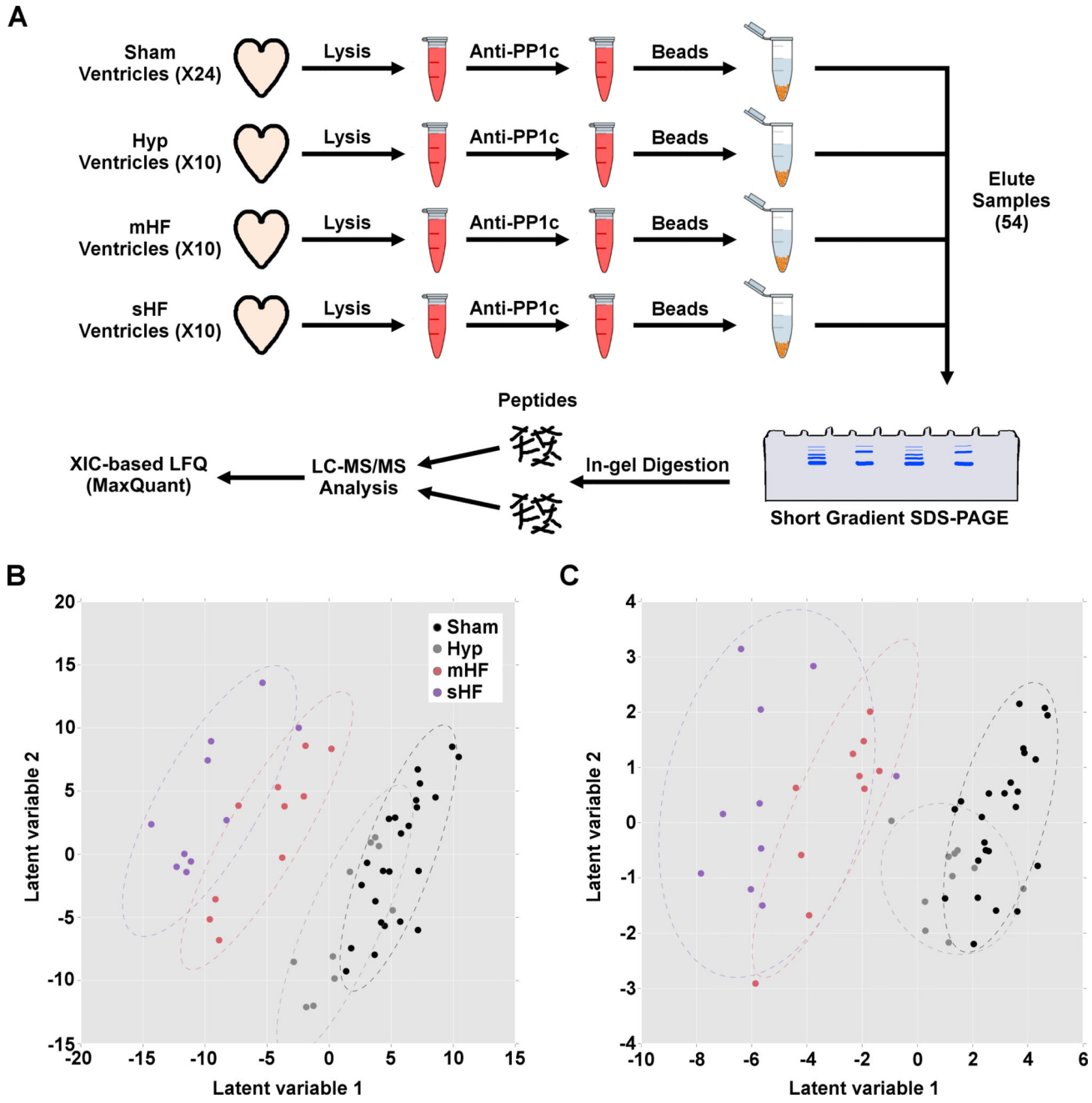

Figure 2. Proteins associated with HF progression

A. Heart tissues from mice in the four groups were processed in parallel. **B.** Quantified proteins from the PP1c AP-MS (692 proteins) were used to build a predictive model using partial least squares (PLS) regression to predict the EF of each animal. Individual dots represent individual samples, and dotted lines show 95% confidence interval for sample group placement. Sham (black) and hypertrophy (Hyp; grey) samples group together, while severe heart failure (sHF; purple) clusters furthest from these groups, with overlap with moderate heart failure (mHF; red). **C.** Repeat PLS regression model using a subset of 40

proteins that were the top predictors of HF progression, identified using forward selection (see Supplemental Figure 3 and Supplemental Table 5).

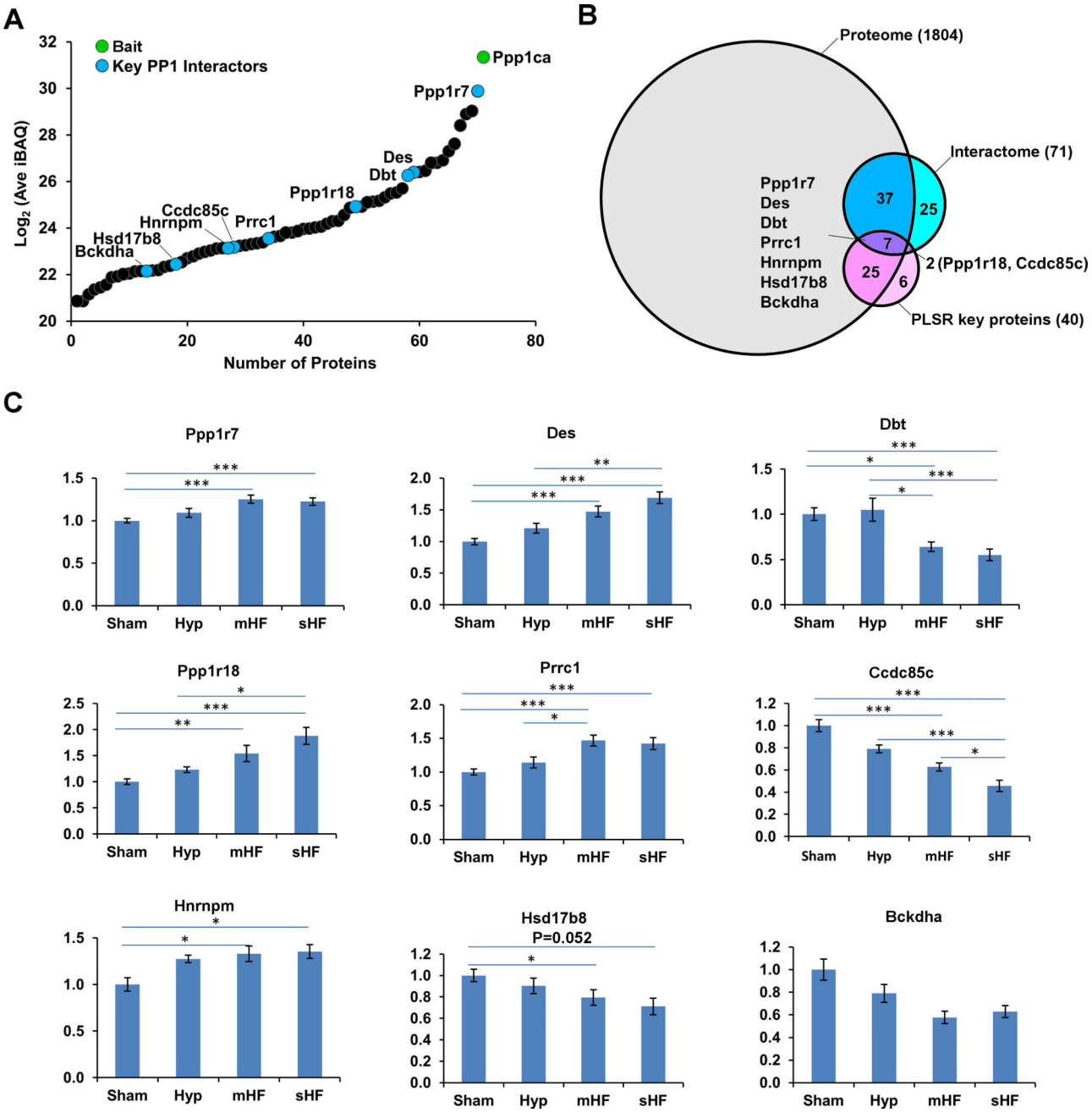

Figure 3. Rearrangement of the PP1 interactome during HF progression

A. Plot of all MS-quantified proteins ranked by relative abundance based on iBAQ values from wild-type heart lysates with PP1c-IP. Key proteins are based on PLS regression model. **B.** Venn diagram showing the overlap of proteins detected without PP1c-IP (“Proteome”), interactors based on PP1c vs. IgG-IPs (“Interactome”), and key proteins that are associated with HF progression as identified by PLS regression. **C.** Levels of binding to PP1c of the 9 key interactors (overlap between “Interactome” and “PLS regression key proteins” from (**B**) during HF progression. *p<0.05, **p<0.01, ***p<0.001.

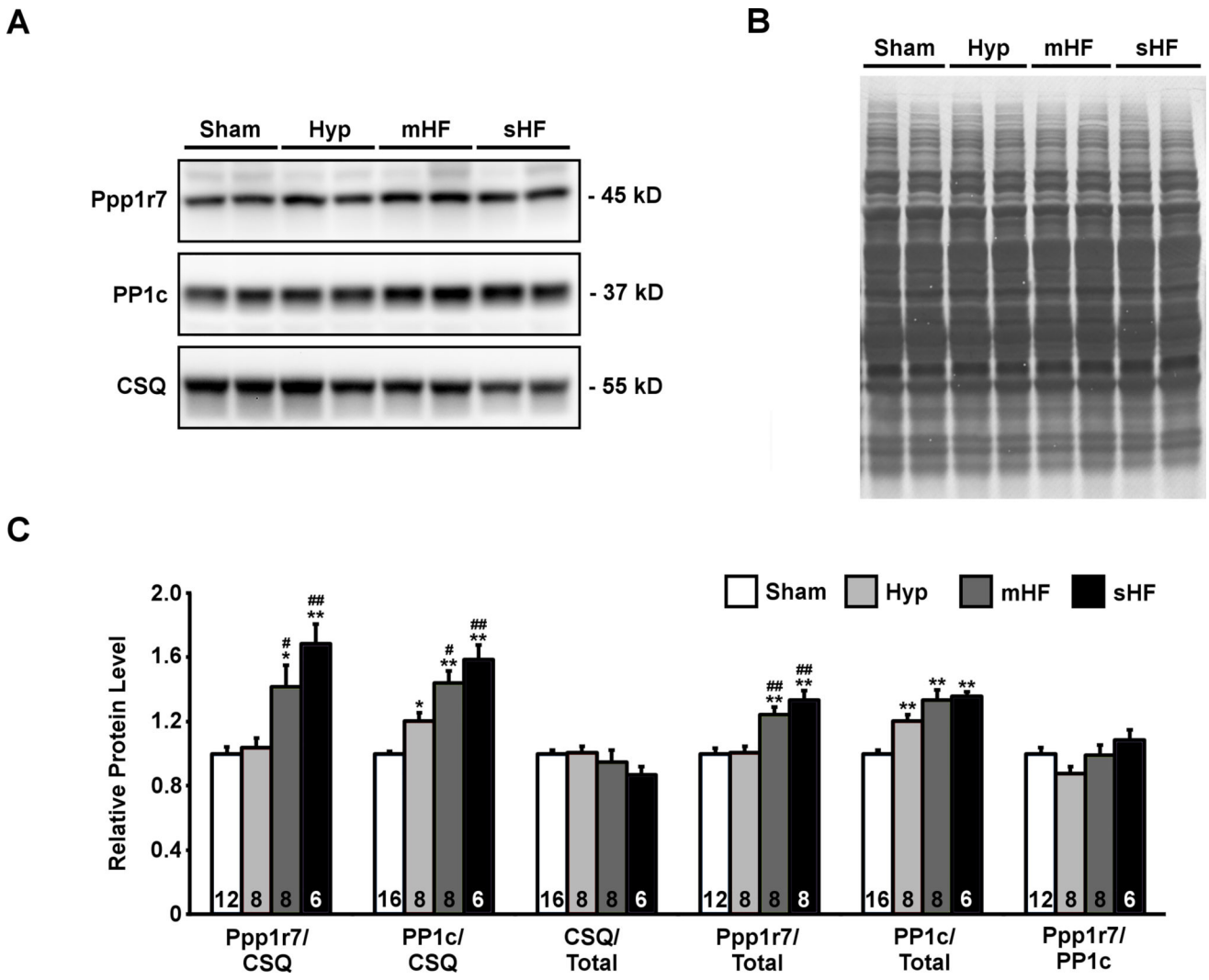

Figure 4. Protein levels of Ppp1r7 during HF progression

Representative western blots (**A**), Coomassie staining showing total protein levels (**B**), and bar graphs (**C**) demonstrating an increase in Ppp1r7 and PP1c normalized to CSQ or total protein levels, but no change in Ppp1r7 normalized to PP1c. Numbers in bars represent numbers of samples. CSQ=calsequestrin. *p<0.05 and **p<0.01 vs. Sham. #p<0.05 and ##p<0.01 vs. Hyp.

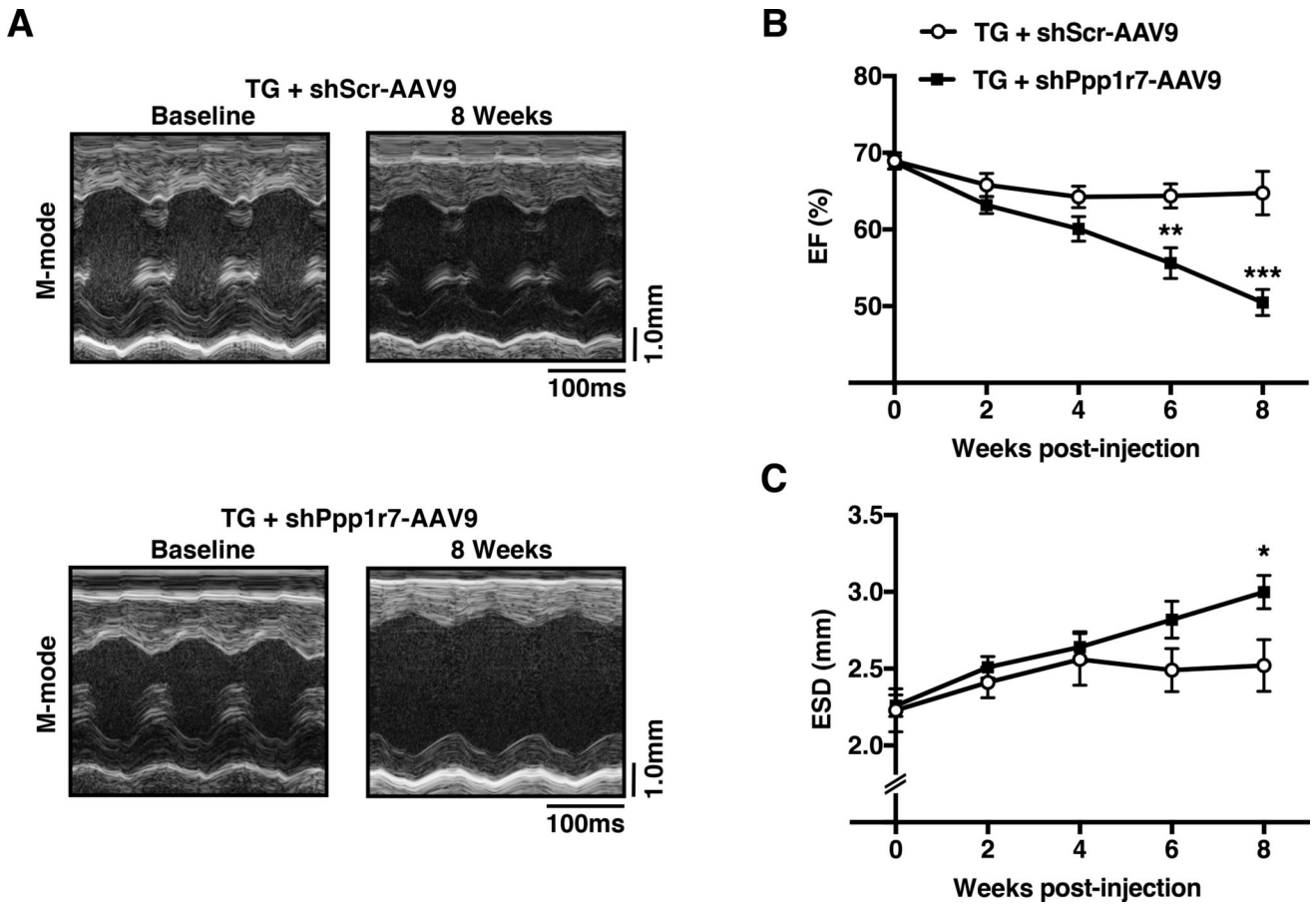

Figure 5. AAV9-mediated knockdown of Ppp1r7 impairs cardiac function *in vivo*

A. Representative M-mode echocardiography tracings from αMHC transgenic (TG) mice at baseline and 8 weeks after injection of either scramble shRNA (shScr)-AAV9 (top) or shRNA targeting Ppp1r7 (shPpp1r7)-AAV9 (bottom). Summary graphs showing (**B**) left ventricular ejection fraction (EF) and (**C**) left ventricular end systolic diameter (ESD) at baseline and 2, 4, 6 and 8 weeks after AAV9 injection. *p<0.05, ***p<0.001 vs. control.

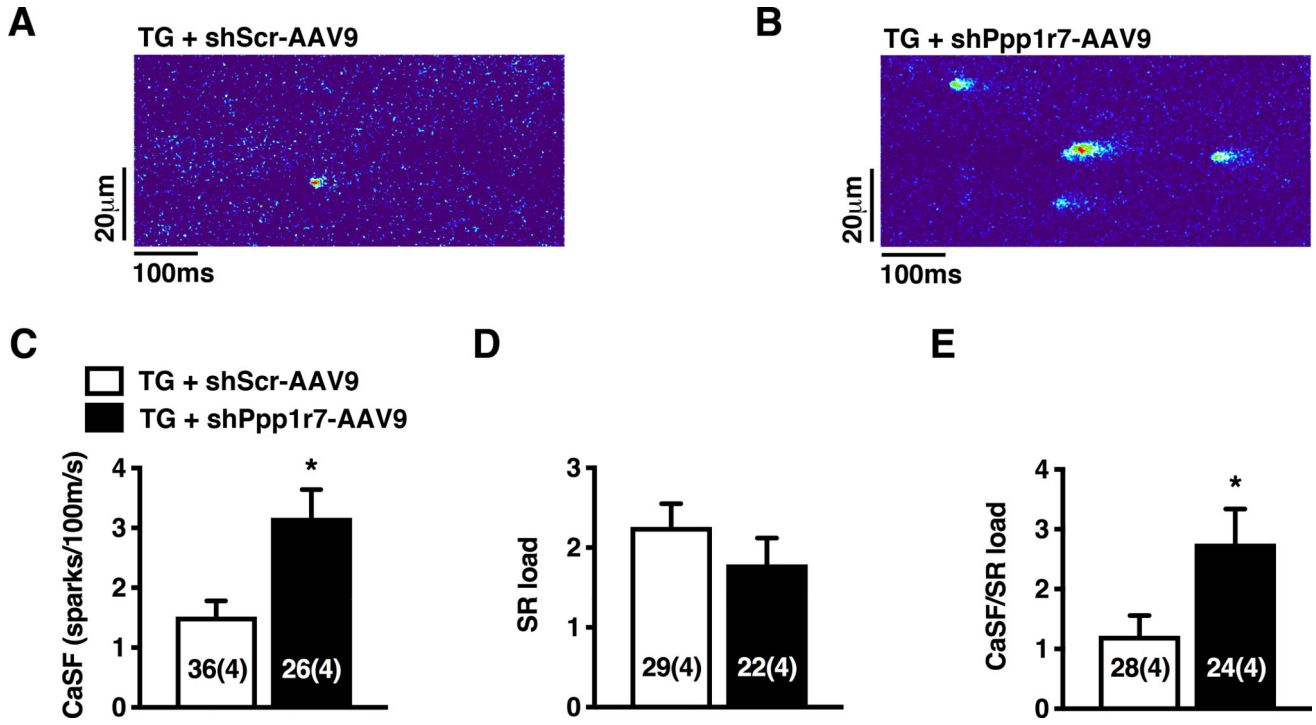

Figure 6. AAV9-mediated Ppp1r7 knockdown impairs calcium handling in ventricular myocytes

A–B. Representative confocal line scan images showing increased number of Ca sparks in myocytes isolated from shPpp1r7-AAV9 treated mice. **C.** Bar graphs showing quantification of Ca sparks frequency (CaSF), (**D**) total sarcoplasmic reticulum Ca content (SR load) and (**E**) CaSF normalized to SR load. *p<0.05 vs. control.

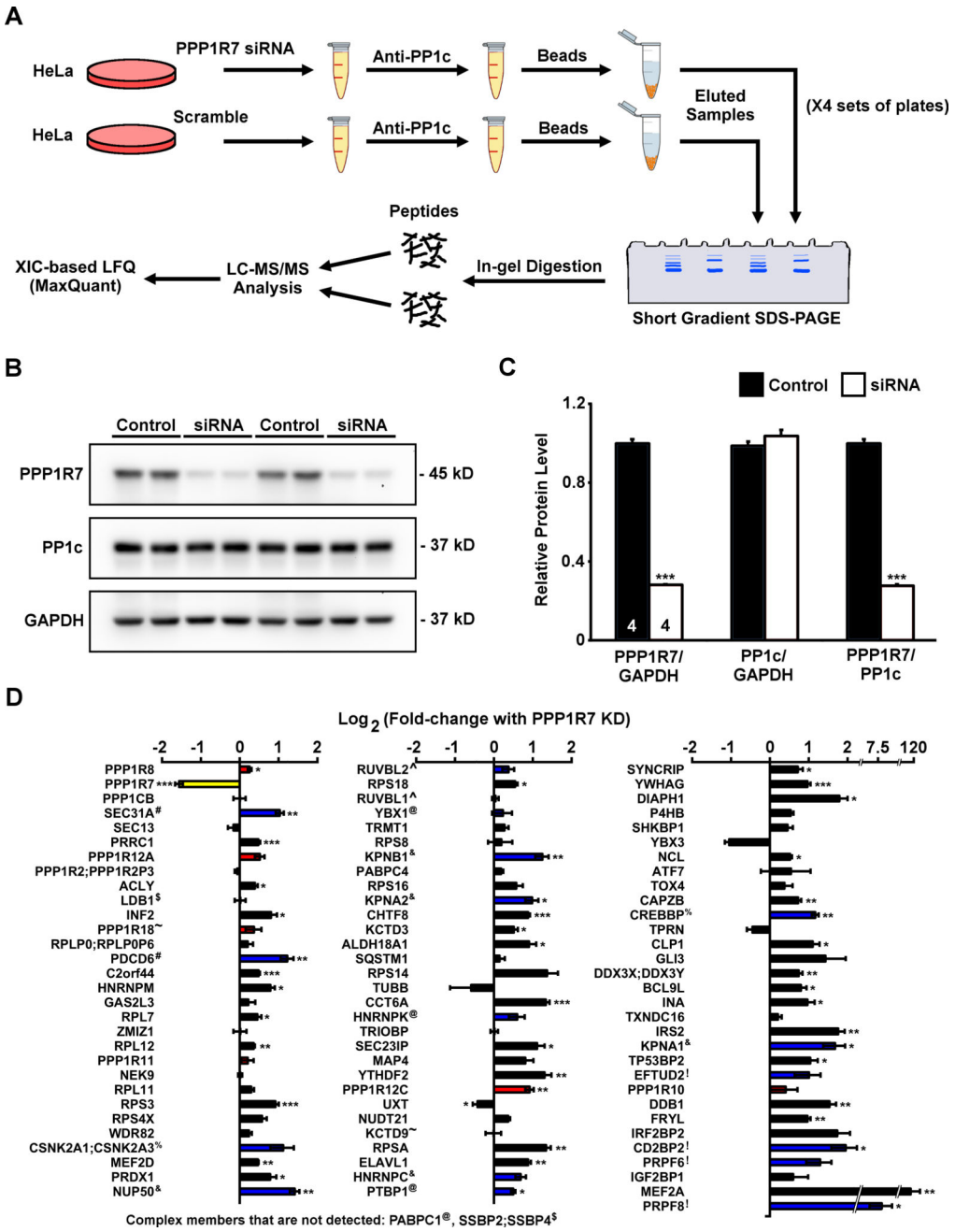

Figure 7. Remodeling of the PP1 interactome with PPP1R7 knockdown

A. Experimental workflow. LC-MS/MS=liquid chromatography-tandem mass spectrometry; XIC=extracted ion chromatogram; LFQ=label free quantitation. **B–C.** Western blots and quantification showing significant knockdown (KD) of PPP1R7 in HeLa cells treated with siRNA. ***p<0.001 vs. control. **D.** Relative changes in the PP1 interactome with PPP1R7 KD. The interactors are ordered from the highest to lowest PP1c-bound based on the HeLa PP1 interactome from the top left to bottom right. Known PP1 subunits are in red and key interactors based on PLS regression are in blue. Proteins with the same symbols (#, $, ~, %,

&, ^, @, !) are in the same complexes based on yeast two-hybrid (Y2H) databases. *p<0.05, **p<0.01, ***p<0.001 vs. control.